THE JOURNAL OF BIOLOGICAL CHEMISTRY VOL. 287, NO. 5, pp. 2971–2983, January 27, 2012
Published in the U.S.A.

Hypokinesia and Reduced Dopamine Levels in Zebrafish Lacking β- and γ1-Synucleins*[S]

Received for publication, September 27, 2011, and in revised form, November 23, 2011 Published, JBC Papers in Press, November 29, 2011, DOI 10.1074/jbc.M111.308312

Chiara Milanese[‡§¶1], Jonathan J. Sager[‡§‖], Qing Bai[‡§], Thomas C. Farrell[‡§], Jason R. Cannon[‡§], J. Timothy Greenamyre[‡§], and Edward A. Burton[‡§**‡‡2]**

*From the [‡]Pittsburgh Institute for Neurodegenerative Diseases and the Departments of [§]Neurology, [‖]Neurobiology, and [‡‡]Microbiology and Molecular Genetics, University of Pittsburgh, Pittsburgh, Pennsylvania 15213, the [¶]Ri.MED Foundation, Palermo 90133, Italy, and the **Geriatric Research, Education and Clinical Center, Pittsburgh Veterans Affairs Healthcare System, Pittsburgh, Pennsylvania 15240*

Background: Synucleins are implicated in Parkinson disease pathogenesis, but their functions are incompletely understood.
Results: Zebrafish lacking β- and γ1-synucleins showed hypokinesia and decreased dopamine levels. These abnormalities were rescued by human α-synuclein.
Conclusion: Synucleins are necessary for spontaneous movement and dopaminergic function.
Significance: A key functional role for synucleins in dopamine neurons may be relevant to Parkinson disease pathogenesis.

α-Synuclein is strongly implicated in the pathogenesis of Parkinson disease. However, the normal functions of synucleins and how these relate to disease pathogenesis are uncertain. We characterized endogenous zebrafish synucleins in order to develop tractable models to elucidate the physiological roles of synucleins in neurons *in vivo*. Three zebrafish genes, *sncb, sncg1*, and *sncg2* (encoding β-, γ1-, and γ2-synucleins respectively), show extensive phylogenetic conservation with respect to their human paralogues. A zebrafish α-synuclein orthologue was not found. Abundant 1.45-kb *sncb* and 2.7-kb *sncg1* mRNAs were detected in the CNS from early development through adulthood and showed overlapping but distinct expression patterns. Both transcripts were detected in catecholaminergic neurons throughout the CNS. Zebrafish lacking β-, γ1-, or both synucleins during early development showed normal CNS and body morphology but exhibited decreased spontaneous motor activity that resolved as gene expression recovered. Zebrafish lacking both β- and γ1-synucleins were more severely hypokinetic than animals lacking one or the other synuclein and showed delayed differentiation of dopaminergic neurons and reduced dopamine levels. Phenotypic abnormalities resulting from loss of endogenous zebrafish synucleins were rescued by expression of human α-synuclein. These data demonstrate that synucleins have essential phylogenetically conserved neuronal functions that regulate dopamine homeostasis and spontaneous motor behavior. Zebrafish models will allow further elucidation of the molecular physiology and pathophysiology of synucleins *in vivo*.

Synucleins are small proteins of 100–140 amino acids that are expressed abundantly in neuronal presynaptic terminals (reviewed in Ref. 1). The three members of the synuclein family, α-, β-, and γ-synuclein, are encoded by separate genes and are widely conserved throughout the vertebrate subphylum. Pathogenic missense (2–4) and gene dose (5, 6) mutations in the *SNCA* gene encoding α-synuclein are an uncommon cause of familial parkinsonism. Convergent lines of evidence suggest that α-synuclein is also centrally involved in the pathogenesis of the common sporadic form of Parkinson disease (PD).[3] The pathological hallmark intraneuronal inclusions of sporadic PD, Lewy bodies, contain insoluble fibrillar aggregates of α-synuclein (7). Furthermore, genome-wide association studies (8–10) show an association between genetic variants at the *SNCA* locus and risk of developing PD. Recent studies support the possibility that *SNCA* variants influencing PD risk may alter α-synuclein expression (11), suggesting that alterations in α-synuclein levels may predispose susceptible neuronal groups to develop pathology in PD. It is currently unclear whether pathogenic involvement of α-synuclein in PD reflects quantitative changes in the activity of its normal cellular functions or the emergence of new pathological functions as its cellular abundance changes. Understanding the normal functions of synucleins is thus an important goal, because this might elucidate aspects of pathogenesis and facilitate identification of therapeutic targets in PD.

Prominent localization of synucleins at presynaptic terminals suggests that they play an important role in synaptic transmission. Mice lacking α-synuclein (12–16), β-synuclein (17), or γ-synuclein (18) show normal development, survival, CNS morphology, synaptic protein expression, synaptic density, and behavior. Changes in the number of dopaminergic neurons (19), striatal dopamine levels and dopamine release (14), and synaptic vesicle pools (16) have been reported in individual

* This work was supported, in whole or in part, by National Institutes of Health Grants NS0583691 and ES019879. This work was also supported by Pittsburgh Foundation Grant M2005-0071 and the Ri.MED Foundation.
[S] This article contains supplemental Tables 1–4.
[1] A Ri.MED scholar.
[2] To whom correspondence should be addressed: Dept. of Neurology, University of Pittsburgh, 7015 BST-3, 3501 Fifth Ave., Pittsburgh PA 15213. Tel.: 412-648-8480; E-mail: eab25@pitt.edu.

[3] The abbreviations used are: PD, Parkinson disease; MO, morpholino oligonucleotide; hpf, hours postfertilization; dpf, days postfertilization; ANOVA, analysis of variance; TAP, tobacco acid pyrophosphatase; IRES, internal ribosome entry site.

Downloaded from http://www.jbc.org/ at ERASMUS MC on March 27, 2018

lines of *SNCA*$^{-/-}$ animals and may reflect variations in genetic background. Synucleins show overlapping expression patterns, raising the possibility that minor abnormalities in single knockout animals are attributable to functional compensation by other synucleins. Mild dopaminergic abnormalities and up-regulation of β-synuclein were found in animals lacking both α- and γ-synucleins (19). Loss of α- and β-synucleins together caused changes in the expression of presynaptic proteins, including up-regulation of γ-synuclein, and a modest reduction in striatal dopamine levels (17). Loss of all three synucleins gave rise to progressive motor impairment; reduced survival; changes in synaptic morphology, physiology, and protein expression; and reduced SNARE complex formation (20, 21) in addition to reduced striatal dopamine content and altered dopamine release (22). These studies show that synucleins are essential for long term maintenance of synapses in the vertebrate CNS, although the molecular basis of these observations and their relevance to Parkinson disease remain undefined. An accessible model allowing mechanistic studies in the intact vertebrate nervous system *in vivo* might be valuable, allowing further definition of the role of synucleins in the molecular physiology of presynaptic terminals.

The zebrafish is a powerful model for studying the vertebrate nervous system. Larvae can be manipulated to be optically transparent, enabling direct visualization of neurons (23, 24), neural circuitry formation (25), and neuronal activity (26, 27) *in vivo*, using transgenically expressed reporter proteins. Zebrafish may also be a useful model in which to study the pathogenesis of neurological disease (reviewed in Refs. 28–30). Importantly, and uniquely among vertebrate models, zebrafish can be subjected to unbiased phenotype-based genetic (31, 32) and chemical (33, 34) screening approaches in order to discover novel molecular insights. The purpose of the present study was to identify and characterize endogenous zebrafish synucleins to allow studies of their functions *in vivo* and to facilitate the development of zebrafish models of Parkinson disease. Here we report that zebrafish do not express α-synuclein. Zebrafish β- and γ1-synucleins are expressed widely in CNS neurons, including dopamine neurons, and are necessary for the development of normal motor and dopaminergic function in zebrafish larvae.

EXPERIMENTAL PROCEDURES

Zebrafish—Experiments were carried out in accordance with National Institutes of Health guidelines and Institutional Animal Care and Use Committee approval. Adult strain AB zebrafish were maintained at 28.5 °C and euthanized by deep tricaine anesthesia followed by exposure to ice-cold water. Embryos were raised in E3 buffer (5 mM NaCl, 0.17 mM KCl, 0.33 mM $CaCl_2$, 0.33 mM $MgSO_4$), supplemented where necessary with 0.003% 1-phenyl-2-thiourea to inhibit pigmentation.

Synteny Analysis—Online tools (NCBI genome viewer and Cinteny (35), both available on the World Wide Web) were used to evaluate syntenic relationships. Proposed orthologues were verified by multiple sequence alignments, and synteny maps were drawn manually.

RT-PCR and 5′-RACE—First strand cDNA was generated by oligo(dT)-primed reverse transcription of total RNA from whole adult zebrafish brains or pooled embryo lysate (SuperScript III, Invitrogen). Nested 5′-RACE was carried out (RLM-RACE, Ambion, Austin, TX) as described previously (24, 36, 37). Primer sequences are listed in supplemental Table 1.

RNA Hybridization and Immunofluorescence—Northen blots (36), whole mount RNA *in situ* hybridization (24), RNA *in situ* hybridization to brain cryosections (24), double label ISH/IHC (38), and indirect immunofluorescence and confocal microscopy (24, 39) were carried out as reported in our previous work. Rabbit anti-α-synuclein (1:300; Santa Cruz Biotechnology, Inc., Santa Cruz, CA) was used to detect human α-synuclein in tissue sections.

Morpholino Oligonucleotides—Antisense morpholino oligonucleotides (MOs; Gene Tools LLC, Philomath, OR) were designed to inhibit zebrafish synuclein gene expression by targeting splice signals in the primary transcripts. Expression of *sncb* was disrupted by MOs targeted against splice donor sites of exons 2 and 3 (*sncb* E2/I2, aatgttgcatgacttacCCACAAAC; *sncb* E3/I3, ttgcagaatcaccttacCTGTTGCA; sequence complementary to the 5′-end of each exon is shown in capital letters). Expression of *sncg1* was disrupted by MOs targeted against the splice donor sites of exons 1 and 3 (*sncg1* E1/I1, tatacatcagcacttacCCACATAC; *sncg1* E3/I3, ctgattgctattcactcacCGGGT). Control MOs (random MO (N_{25}) and non-targeting MO CCTCTTACCTCAGTTACAATTTATA) were used to exclude nonspecific effects arising from morpholino exposure. 3 nl of MO dissolved in 1× Danieau Buffer (58 mM NaCl, 0.7 mM KCl, 0.4 mM $MgSO_4$, 0.6 mM $Ca(NO_3)_2$, 5.0 mM HEPES, pH 7.6) was injected into the yolk sac at the 1–2-cell stage. For *sncb*, 3 ng of *sncb* E3/I3 MO and 5 ng of *sncb* E2/I2 MO were injected (β MO). For *sncg1*, 4 ng of each *sncg1* E1/I1 and *sncg1* E3/I3 were injected (γ1 MO). To target both *sncb* and *sncg1*, all four MOs were injected (β + γ1 MO), total dose 14 ng. Control MO was injected at 14 ng/embryo.

mRNA Rescue—A NotI/XhoI fragment of pIRES2-EGFP (Clontech, Mountain View, CA) was inserted into the XbaI/XhoI sites of pCS2$^+$ (40) to generate plasmid pCS-IG. Human α-synuclein cDNA was amplified from NT2 cells by RT-PCR, sequenced, and inserted into the XhoI/XmaI sites of pCS-IG to generate pCS-syn-IG. pCS-IG and pCS-syn-IG were linearized at the NotI site 3′ to the poly(A) signal, and mRNA was transcribed from the Sp6 promoter (mMessage Machine, Ambion, Austin, TX). Intracellular injection of 1–1.25 nl of mRNA solution (250 pg/nl mRNA, 0.25% phenol red, 120 mM KCl, 20 mM HEPES, pH 7.4) was carried out at the single cell stage, followed by MO injection into the yolk sac as above.

Western Blot—Western blots were carried out as described previously (36, 39). Proteins were transferred to PVDF membrane (Immobilon, Millipore, Billerica, MA), and blots were blocked in Odyssey Blocking Buffer (LI-COR, Lincoln, NE). Primary antibodies were as follows: α-synuclein (mouse; 1:1000; BD Biosciences) and β-actin (rabbit; 1:2000; Sigma). Secondary antibodies conjugated to different infrared fluorophores (anti-mouse IRdye®800 and anti-rabbit IRdye®680; 1:10,000 each; LI-COR) allowed simultaneous detection of both proteins using a two-channel infrared imaging system (LI-COR).

Motor Analysis—Larval movement was analyzed using a proprietary system (Zebralab; ViewPoint Life Sciences, Montreal,

Downloaded from http://www.jbc.org/ at ERASMUS MC on March 27, 2018

Canada) as reported previously (34). Zebralab software was used in "quantization mode" with detection sensitivity set to 16 and with burst and freezing activity thresholds set to 10 and 2, respectively. Groups of 15 embryos were analyzed in 12-well plates containing 3 ml of E3 buffer/well. Spontaneous activity was measured for an 8-h period daily, from 24 h postfertilization (hpf) to 7 days postfertilization (dpf).

Neurochemical Measurements—Neurochemical measurements were performed by adapting a previously reported method (41). 30 larvae were sonicated in 150 μl of 4 M perchloric acid, 0.1% $Na_2S_2O_5$, 0.1% EDTA at 4 °C. The sample was centrifuged at 17,000 × *g* at 4 °C, and the supernatant was filtered through a 0.22-μm nylon membrane (Spin-X, Corning Glass). 25 μl was loaded into a Waters 2695 HPLC separation module (Waters, Milford, MA). The HPLC mobile phase consisted of 0.06 M sodium phosphate monobasic, 0.03 M citric acid, 8% methanol, 1.1 mM 1-octanesulfonic acid, 0.1 mM EDTA, 2 mM sodium chloride, pH 3.5. The flow rate was 1.0 ml/min. Neurotransmitters were separated on a Waters XBridge C18 4.6 × 150-mm column, particle size 3.5 μm, at 34 °C, and detected using a Waters 2465 electrochemical detector with a glassy carbon electrode set at 750 mV, referenced to an ISAAC electrode. Neurotransmitters were quantified as pg/larva, using a standard curve generated from injection of high purity standards. Each data point was then normalized to the value for wild type animals in the same experiment.

Statistical Analysis—Quantitative data were shown to be normally distributed by Pearson's and D'Agostino's tests and were analyzed using parametric statistical tests. All experiments were repeated at least in triplicate. Graphs show means ± S.E. One-way ANOVA was carried out after confirming the assumption of equal variance using Bartlett's test and was followed by Dunnett's post hoc test to evaluate statistically significant differences between test groups.

RESULTS

Zebrafish Synucleins—Identification of zebrafish synucleins was recently reported by two other groups (42, 43). We independently cloned the same genes at the start of this study (not shown). *sncb* encodes the zebrafish orthologue of human β-synuclein, and *sncg1* and *sncg2* encode dual paralogues of human γ-synuclein. Zebrafish synucleins show extensive sequence similarity to human synucleins, except that the C termini of the two zebrafish γ-synucleins are relatively divergent (Fig. 1). We did not identify an orthologue of human α-synuclein in zebrafish genomic, mRNA, or expressed sequence tag databases, which was unexpected because α-synuclein orthologues have been identified in mammals, birds, reptiles, amphibians, and other fish species. Despite employing a variety of RT-PCR and RACE strategies to amplify a putative *snca* transcript (supplemental Table 4), we did not find evidence of a zebrafish α-synuclein orthologue expressed in the CNS.

In order to further understand how human and zebrafish synuclein genes are related, we constructed synteny maps (Fig. 2). Two of the genes flanking the *sncb* gene on zebrafish chromosome 13 are orthologues of genes flanking the human *SNCB* gene on chromosome 5 (Fig. 2*A*), suggesting that the genes are derived from a common ancestral locus. A large genomic

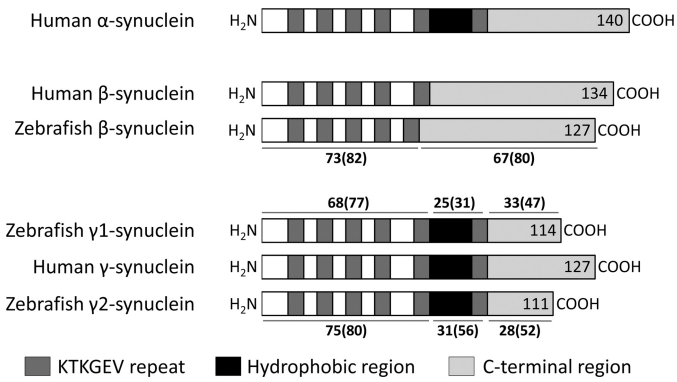

FIGURE 1. **Zebrafish synucleins.** The structures of zebrafish β-, γ1-, and γ2-synucleins are shown schematically in comparison with human synucleins to illustrate the conserved structure of the proteins. The N-terminal KTKGEV repeats, hydrophobic region, and C-terminal acidic region are shown. The number of amino acids in each protein is shown at its C terminus. The percentage of amino acid identity (and similarity in *parentheses*) between the indicated regions of the human and zebrafish proteins is annotated. Sequence alignments and detailed annotations are shown in the supplemental material.

region surrounding zebrafish *sncg1* and *sncg2* is duplicated and is syntenic with the human genomic region containing *SNCG* (Fig. 2*B*). These observations suggest that *sncg1* and *sncg2* are derived from duplication of an ancestral locus shared with human *SNCG*. Zebrafish orthologues of genes immediately flanking human *SNCA* were not found in the available zebrafish genome sequence, whereas the wider genomic region in the human showed two blocks of genes that were syntenic to different regions of the zebrafish genome (Fig. 2*C*). It is possible that the region between these syntenic blocks was deleted from an ancestral chromosome during evolution, accounting for the lack of zebrafish genomic or mRNA sequences with homology to human *SNCA*.

mRNA Transcripts and Genomic Organization of Zebrafish Synucleins—Zebrafish *sncb* and *sncg1* transcripts were detected abundantly in adult brain by Northern blot (Fig. 3*A*). Each gene gave rise to a single mRNA species of 1.45 kb (*sncb*) or 2.7 kb (*sncg1*). *sncg2* was alternatively spliced to yield two transcripts encoding isoforms with divergent C termini; although both transcript variants were amplified from CNS by PCR (Fig. 3*B*), we were unable to identify *sncg2* transcripts in the CNS by Northern blot hybridization or RNA *in situ* hybridization and conclude that they are present at low abundance. The remainder of this study focused on *sncb* and *sncg1*, encoding the predominant CNS synucleins in zebrafish.

5′-RACE (Fig. 3*C*), using the tobacco acid pyrophosphatase (TAP) method (as described previously (24, 36, 37)), was employed to map the 5′-ends of the *sncb* and *sncg1* transcripts. TAP^- and RT-PCR controls verified that the boundary between the RACE adapter and the cDNA sequence in the RACE products occurred at the mRNA cap site. Both *sncb* and *sncg1* promoter regions lack canonical TATA motifs and show multiple transcriptional start sites from motifs with homology to the initiator consensus 5′-YYA^{+1}NWYY-3′ (44) (Fig. 3, *D* and *E*). We next examined the genomic organization of *sncb*, *sncg1*, and *sncg2* by comparing cDNA sequences with the zebrafish genomic sequence (Fig. 3, *F–H*, and supplemental Tables 2 and 3). Like its human orthologue, *sncb* contains six exons, the first of which is non-coding. Similar to their human

Downloaded from http://www.jbc.org/ at ERASMUS MC on March 27, 2018

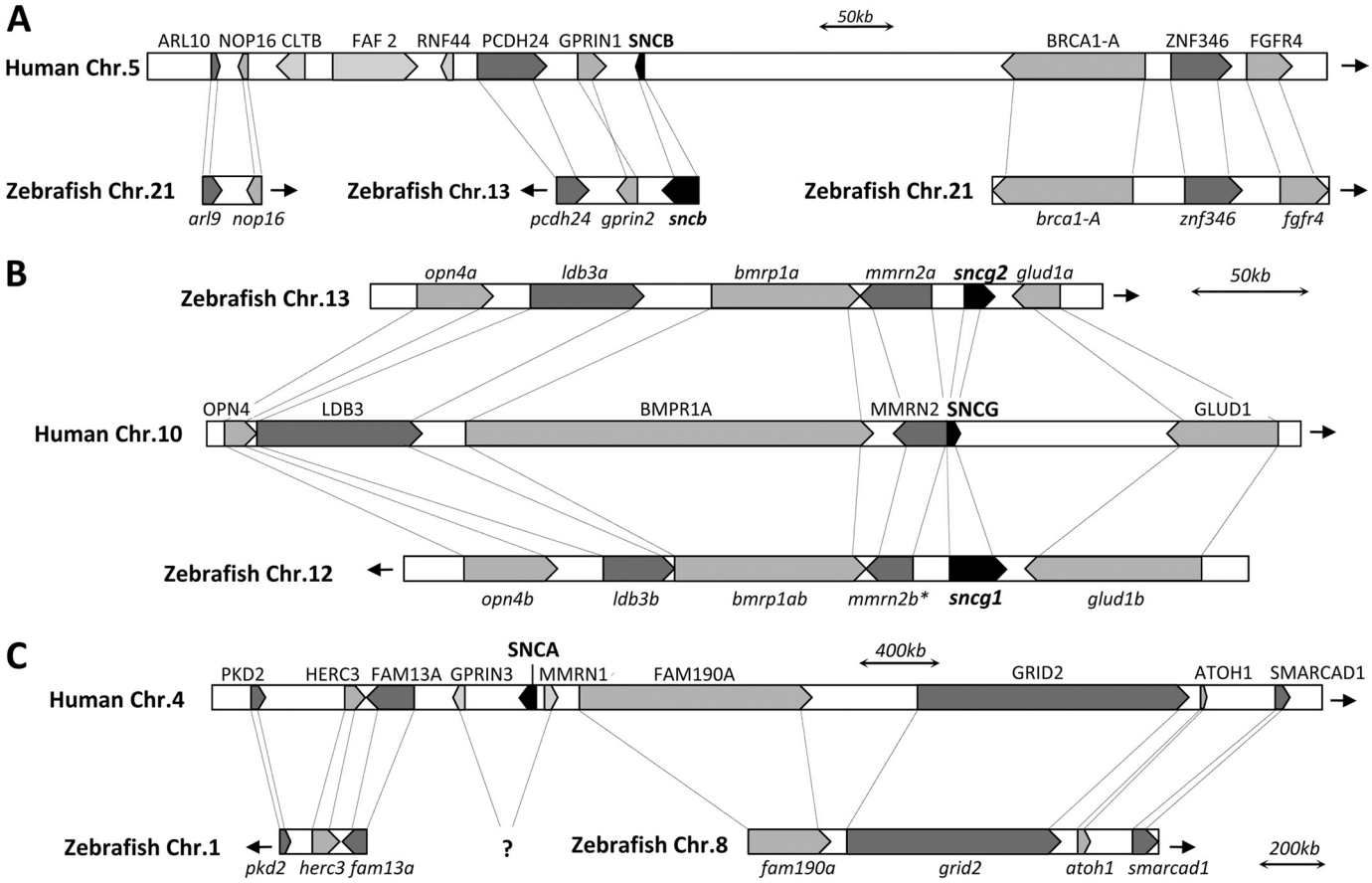

FIGURE 2. **Analysis of human-zebrafish synteny adjacent to genes encoding synucleins.** Paralogues of the genes flanking human synuclein genes (*SNCB* (*A*), *SNCG* (*B*), and *SNCA* (*C*)) were identified in the zebrafish. The diagrams depict syntenic relationships between the relevant segments of the zebrafish and human genomes. Each chromosome is labeled to its *left*, and the direction of the telomere is indicated by an *arrow*. Genes are shown approximately to scale. Paralogues are *shaded* the same *color* and are related to one another by *dashed lines*. Synuclein genes are *shaded black* and labeled in *boldface type*. No orthologue of human *SNCA* or its flanking genes *GPRIN3* and *MMRN1* was found in the zebrafish genome.

paralogue, both *sncg1* and *sncg2* contain five exons. The positions and phases of the splice boundaries in *sncb*, *sncg1*, and *sncg2* are conserved with respect to their human paralogues, providing further evidence of a common origin (supplemental material).

Expression Patterns of Zebrafish Synucleins—The expression patterns of zebrafish synucleins were determined by RNA *in situ* hybridization. As reported previously during early development (42, 45), *sncb* and *sncg1* were expressed in the CNS, whereas *sncg2* was found in the notochord (Fig. 4, *A*–*C*). In the adult zebrafish CNS, both *sncb* and *sncg1* were expressed in cells with neuronal morphology, widely distributed throughout gray matter of the brain and spinal cord. However, their topographical expression patterns differed significantly; *sncb* was more robustly expressed rostrally, whereas *sncg1* expression was more prominent caudally (Fig. 4, *D* and *E*). Differences in the expression patterns of *sncb* and *sncg1* in specific brain regions are illustrated in Fig. 4*F*. Whereas prominent *sncb* expression was detected in the olfactory bulb and dorsal telencephalon, *sncg1* was not expressed at high levels in these regions. Conversely, robust *sncg1* expression in the medulla oblongata and habenula was accompanied by weak expression of *sncb* in these areas. Even within some brain regions where there was overlap between *sncb* and *sncg1* expression, the two genes were expressed in different cellular populations. For example, within the cerebellum, *sncb* was expressed within granule cells, whereas *sncg1* was expressed most prominently in the Purkinje cell layer (Fig. 4*G*).

We next examined expression of *sncb* and *sncg1* in catecholaminergic neurons in the zebrafish CNS. In the absence of available antibodies to zebrafish β- or γ1-synucleins, we used a double label ISH/IHC technique, allowing us to detect *sncb* or *sncg1* and tyrosine hydroxylase simultaneously in the same tissue sections. Examples are shown in Fig. 4*H*; dopaminergic neurons of the periventricular hypothalamus were identified by their morphology and by robust tyrosine hydroxylase immunoreactivity in their processes. Strong expression of *sncb* (Fig. 4*H*, *left*) and *sncg1* (*right*) was also evident in the perinuclear cytoplasm. Using this method, we examined each of the major catecholaminergic cell groups within the olfactory bulb, telencephalon, diencephalon, and hindbrain. With the exception that *sncg1* expression was relatively weak in the olfactory bulb, all tyrosine hydroxylase-immunoreactive groups also expressed both *sncb* and *sncg1*. These data suggest that *sncb* and *sncg1* may be co-expressed in catecholaminergic neurons.

β- and γ1-Synucleins Are Not Required for Early Embryogenesis or CNS Morphogenesis—We next asked whether perturbing expression of *sncb* or *sncg1* using antisense MOs would result in a neurodevelopmental phenotype that might be

Downloaded from http://www.jbc.org/ at ERASMUS MC on March 27, 2018

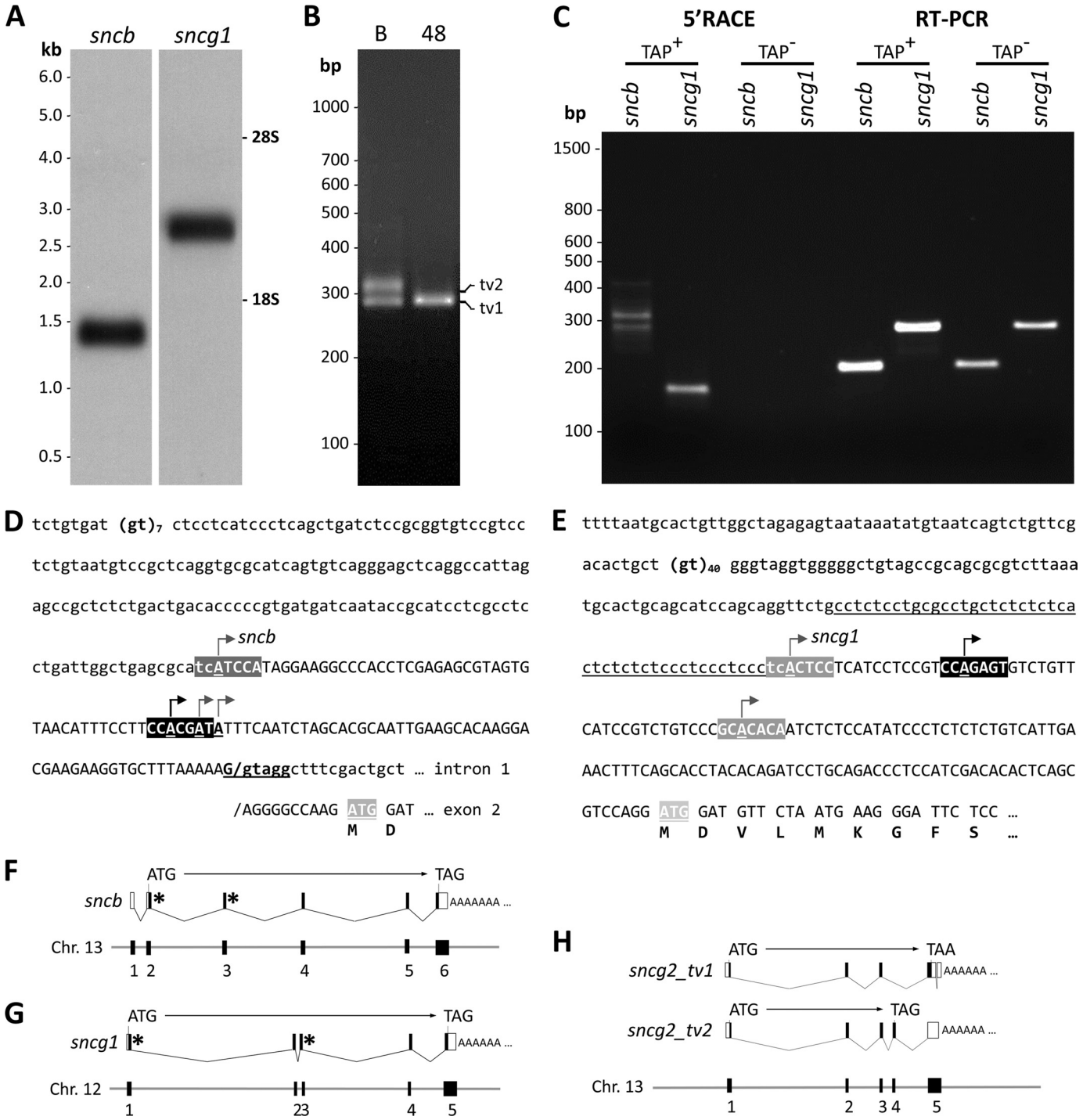

FIGURE 3. **Zebrafish synucleins: transcripts, promoters, and genomic organization.** *A*, Northern blots containing total RNA from adult zebrafish brain were hybridized with cRNA probes complementary to *sncb* (*left*) or *sncg1* (*right*). The positions of molecular size markers (kb) are shown to the *left* of the blots, and the positions of the 28 and 18 S ribosomal RNA bands are shown to the *right*. *B*, total RNA derived from adult brain or embryos at 48 hpf was subjected to RT-PCR using primers complementary to exons 3 and 5 of *sncg2*. The picture shows an ethidium-stained agarose gel under UV illumination following electrophoretic separation of the products. Bands corresponding to *sncg2* tv1 (lacking exon 4) and *sncg2* tv2 (containing exon 4) are labeled to the *right* of the *picture*. *C*, 5′-RACE was used to map the transcriptional start sites of *sncb* (*lanes 1*, *3*, *5*, and *7*) and *sncg1* (*lanes 2*, *4*, *6*, and *8*). The picture shows an ethidium-stained agarose gel under UV illumination following electrophoretic separation of PCR products. 5′-RACE (*lanes 1–4*) and RT-PCR (*lanes 5–8*) were carried out using cDNA template derived from samples in which RNA was either treated with tobacco acid pyrophosphatase (TAP^+; *lanes 1*, *2*, *5*, and *6*) or received no treatment (TAP^-; *lanes 3*, *4*, *7*, and *8*) prior to adapter ligation. *D* and *E*, the promoter regions of *sncb* (*D*) and *sncg1* (*E*) are shown. The *arrows* indicate transcriptional start sites identified by 5′-RACE; initiator sequences are *highlighted* in *gray*, and the major start sites of each transcript are *highlighted* in *black*. The splice donor consensus of *sncb* exon 1 is *underlined*. A pyrimidine-rich sequence in the *sncg1* 5′-flanking region is *underlined*. *F–H*, the genomic organization of *sncb* (*F*), *sncg1* (*G*), and *sncg2* (*H*) are shown schematically. The *lower part* of each diagram depicts the genomic sequence showing the position and number of each exon. The *upper part* shows the major transcripts arising from each gene and the locations of the open reading frames (*shaded* in *black* and labeled *ATG→TAG*). *, splice donor sequences in *sncb* and *sncg1* that were targeted by antisense morpholino oligonucleotides.

Downloaded from http://www.jbc.org/ at ERASMUS MC on March 27, 2018

informative regarding the normal functions of β- and γ1-synucleins. Antibodies to zebrafish synucleins are not available, so verification of translation-inhibiting MOs was not possible; consequently, we inhibited gene expression by targeting pre-mRNA splice sites because splicing could be verified by RT-PCR. Pairs of MOs targeting two splice boundaries in each transcript greatly reduced expression, such that *sncb* or *sncg1* mRNA could not be detected by RT-PCR up to 72 hpf (Fig. 5, *A* and *B*). We refer to the pair of MOs targeting *sncb* as β MO and the pair of MOs targeting *sncg1* as γ1 MO. As a control for nonspecific effects of MOs, we used both non-targeting and random MOs (termed *Ctrl MO* in subsequent figures) at the

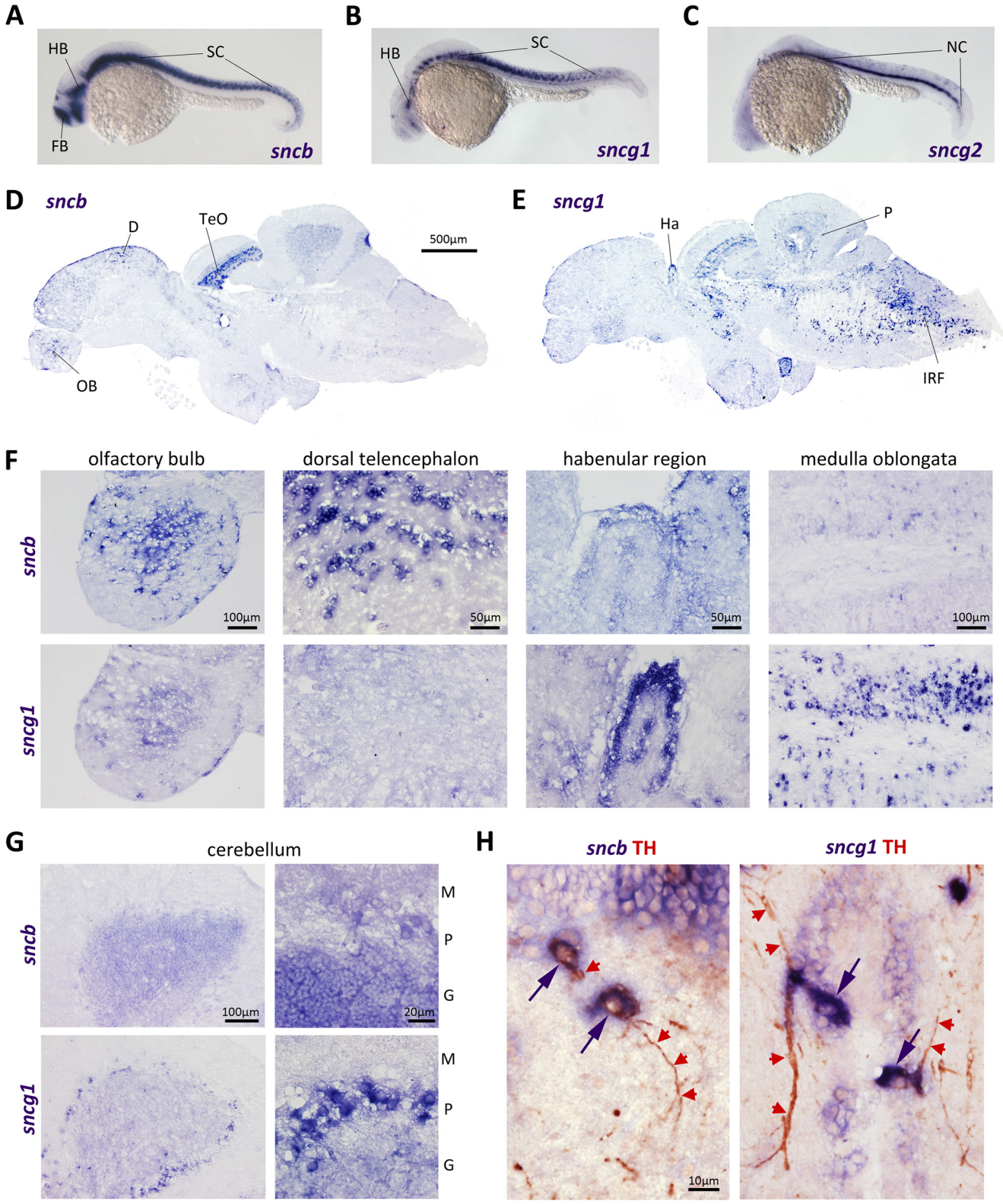

Downloaded from http://www.jbc.org/ at ERASMUS MC on March 27, 2018

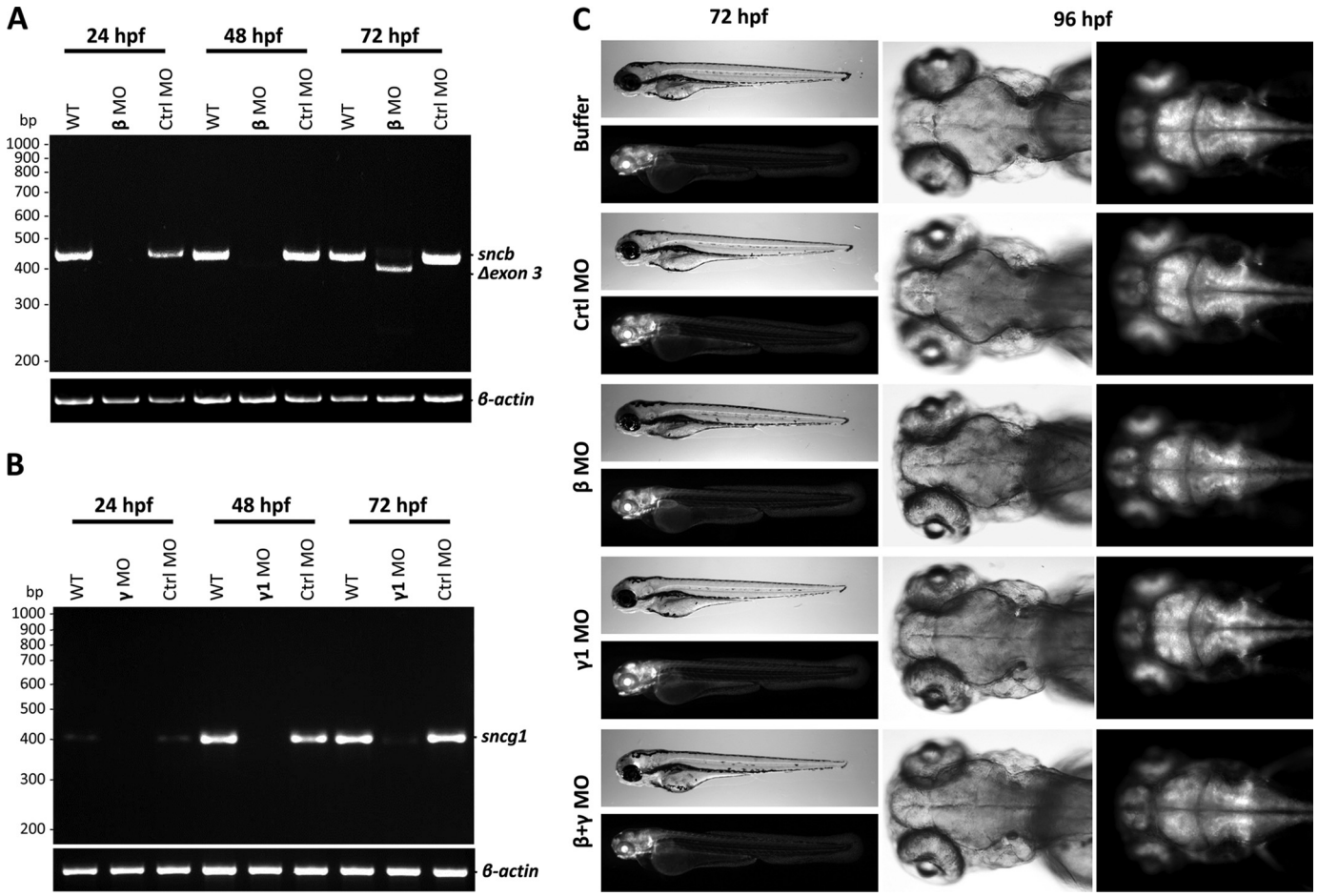

FIGURE 5. **Morpholino oligonucleotides targeting expression of *sncb* and *sncg1* during development.** *A*, morpholino oligonucleotide targeting of *sncb*. RNA was harvested from zebrafish embryos at 24 (*lanes 1–3*), 48 (*lanes 4–6*) and 72 hpf (*lanes 7–9*) and subjected to RT-PCR analysis using primers to *sncb* (*top*) or *bactin1* (*bottom*). The images show UV-illuminated ethidium-stained agarose gels following electrophoretic separation of the PCR products. Uninjected embryos (*WT*; *lanes 1*, *4*, and *7*) were compared with embryos injected at the single cell stage with MOs targeting the splice donor sequences of exons 2 and 3 of the primary *sncb* transcript (*β MO*; *lanes 2*, *5*, and *8*) or a non-targeting control MO (*Ctrl MO*; *lanes 3*, *6*, and *9*). The positions of molecular size markers (bp) are shown to the *left* of the image. The positions of bands corresponding to *sncb* mRNA and an *sncb* transcript lacking exon 3 are labeled to the *right* of the image. *B*, morpholino oligonucleotide targeting of *sncg1*. RNA was harvested from zebrafish embryos at 24 (*lanes 1–3*), 48 (*lanes 4–6*), and 72 hpf (*lanes 7–9*) and subjected to RT-PCR analysis using primers to *sncg1* (*top*) or *bactin1* (*bottom*). Uninjected embryos (*WT*; *lanes 1*, *4*, and *7*) were compared with embryos injected at the single cell stage with MOs targeting the splice donor sequences of exons 1 and 3 of the primary *sncg1* transcript (*γ1 MO*; *lanes 2*, *5*, and *8*) or a non-targeting control MO (*Ctrl MO*; *lanes 3*, *6*, and *9*). *C*, morphology of zebrafish lacking *β*- or γ1-synuclein. Zebrafish embryos were injected at the single cell stage with injection buffer only (*buffer*), a non-targeting control MO (*Ctrl MO*), or MOs targeting *sncb* (*β MO*), *sncg1* (γ1 *MO*), or both *sncb* and *sncg1* (*β* + *γ1 MO*). Bright field lateral images of larvae at 72 hpf and dorsal views of the head region are shown alongside epifluorescence images from Tg(*eno2:egfp*) (24) larvae at the same time points in order to show the structure of the CNS.

same concentrations. These did not affect expression of either *sncb* or *sncg1* (Fig. 5, *A* and *B*).

Zebrafish lacking *β*-, γ1-, or both synucleins were viable and showed normal development of the basic body plan, internal organs, and circulation (Fig. 5*C*). In order to examine the morphology of the nervous system in more detail, we employed Tg(*eno2:egfp*) zebrafish, which express GFP in a pan-neuronal pattern (24), allowing delineation of CNS structure and exam-

FIGURE 4. **Expression of zebrafish synucleins during development and in the adult CNS.** *A–C*, whole mount RNA *in situ* hybridization was carried out in zebrafish embryos at 24 hpf using cRNA probes to *sncb* (*A*), *sncg1* (*B*), or *sncg2* (*C*). Hybridized probe was revealed using a chromogenic substrate with a *purple/blue* reaction product. Structures expressing each transcript are labeled. *FB*, forebrain; *HB*, hindbrain; *SC*, spinal cord; *NC*, notochord. *D* and *E*, RNA *in situ* hybridization was carried out on parasagittal sections from fixed adult brains using cRNA probes specific to *sncb* (*D*) and *sncg1* (*E*). Hybridized probe was revealed using a chromogenic substrate with a *purple/blue* reaction product. The images show low magnification micrographs to illustrate the topographical expression patterns of the transcripts. The scale for both images is shown to the *right* of *D*. Structures expressing each transcript are labeled in each image. *OB*, olfactory bulb; *D*, dorsal telencephalon; *TeO*, optic tectum; *Ha*, habenula; *P*, cerebellar Purkinje cell layer; *IRF*, inferior reticular formation. *F* and *G*, adult brain sections processed identically to those shown in *D* and *E* are shown at higher magnification in order to illustrate regions in which *sncb* (*top row*) and *sncg1* (*bottom row*) showed different expression patterns. The anatomical region is labeled *above* each pair of images, and the scale for both micrographs is shown in the *upper* of the two. In *G*, the cerebellum is shown at two different magnifications. *M*, molecular layer; *P*, Purkinje cell layer; *G*, granule cell layer. *H*, *two-color* RNA *in situ* hybridization/immunohistochemistry (38) was used to examine expression of synuclein mRNAs in dopaminergic neurons. In each image, RNA *in situ* hybridization was carried out using cRNA probes complementary to *sncb* (*left*) or *sncg1* (*right*), and hybridized probe was detected using a chromogenic reaction with a *blue/purple* product. The sections were then labeled using an antibody to tyrosine hydroxylase (64), and bound antibody was detected using a second chromogenic reaction with a *red* product. Examples are shown of dopaminergic neurons in the periventricular hypothalamus that showed expression of *sncb* or *sncg1* mRNA in their cell bodies (*purple arrows*) and tyrosine hydroxylase (*TH*) in their processes (*red arrows*). The scale for both images is shown in the *lower right corner* of the *left panel*.

Downloaded from http://www.jbc.org/ at ERASMUS MC on March 27, 2018

ination of spinal morphology and nerve roots. Compared with controls, we did not detect any abnormalities of CNS or PNS structure in Tg(*eno2*:*egfp*) larvae lacking β-, γ1-, or both synucleins. In particular, the CNS appeared structurally unremarkable at 4 dpf, the time point at which the most robust neurobehavioral abnormalities were found (see below). These data show that β- and γ1-synucleins are not necessary for development of normal CNS morphology.

β- and γ1-Synucleins Are Required for Normal Development of Motor Function—To evaluate the role of β- and γ1-synycleins in neuronal function, we employed an assay of spontaneous larval movement. A live video stream showing zebrafish larvae housed in multiwell plates was analyzed for movement by quantifying the changes in pixel gray scale values that accompany larval displacement from frame to frame. In order to detect changes in the frequency with which spontaneous movements were executed, we measured the proportion of video frames in which pixel gray scale changes exceeded the threshold for detection of movement above stochastic pixel noise. To confirm that this method could quantify spontaneous movement under the conditions used for our study, we housed 0, 2, 4, 8, or 16 zebrafish in each well of a 12-well plate and quantified motor activity at 2, 3, and 7 dpf (Fig. 6*A*). No movement was detected in empty wells, and the relationship between the number of larvae in a well and measured motor activity was linear.

We next analyzed movement of groups of 15 larvae from each experimental group (WT, buffer-injected, Ctrl MO, β MO, γ1 MO, or β + γ1 MO). Six independent experimental replicates were carried out at each time point between 2 and 7 dpf (Fig. 6*B*). In uninjected larvae, little movement was detected at early developmental points; however, motor activity increased sharply at 4 dpf and remained at approximately the same level until 7 dpf. At each time point, there were no statistically significant differences between uninjected larvae, larvae injected with buffer only, and larvae injected with control MOs at the highest doses used in gene targeting experiments. Thus, neither the mechanical consequences of microinjection nor nonspecific toxic effects of exposure to MOs induced changes in spontaneous movement in this assay. At 2 dpf, small statistically significant reductions in activity were apparent between controls and larvae lacking β-, γ1-, or both synucleins, but these changes resolved by 3 dpf. Between 3 and 4 dpf, larvae lacking β- or γ1-synucleins showed only a modest increase in activity, compared with the large increase seen in controls. Consequently, at 4 dpf, larvae lacking β- or γ1- synucleins showed a robust reduction in spontaneous movement compared with controls. Loss of motor activity was more severe in larvae lacking both β- and γ1-synucleins than in larvae lacking one or other synuclein. As gene expression recovered later in development, the hypokinetic phenotype started to resolve. By 5 dpf, spontaneous movement in synuclein knockdown animals had almost returned to control levels, and only animals injected with β + γ1 MO showed statistically significant differences from controls. By 7 dpf, the groups were statistically indistinguishable, although measured motor activity remained lower in larvae exposed to β + γ1 MO than in the other experimental groups.

In order to firmly establish whether these motor abnormalities were attributable to loss of synucleins, we next asked whether this hypokinetic phenotype could be rescued by an exogenous synuclein. Human α-synuclein was expressed in zebrafish embryos by microinjecting a bicistronic mRNA encoding both α-synuclein and GFP. mRNA encoding GFP alone was used as a control. Because the IRES element functions weakly in zebrafish (not shown), human α-synuclein expression was verified by other methods. Western blot showed a single 16-kDa α-synuclein immunoreactive band specific to microinjected embryos; immunofluorescence demonstrated robust α-synuclein expression throughout microinjected embryos, including the neural tube and developing retina (Fig. 6*C*). Expression of either GFP or human α-synuclein did not alter WT larval motor activity (Fig. 6*D*). Reduced motor activity at 4 dpf was seen in GFP-expressing larvae lacking β-, γ1-, or β- and γ1-synucleins, similar to results in larvae expressing no exogenous mRNA. In contrast, animals expressing human α-synuclein showed normal levels of motor activity in the absence of β- or γ1-synuclein. In the absence of both β- and γ1-synucleins, it was necessary to express a higher level of human α-synuclein in order to prevent loss of spontaneous movement. These data show that the hypokinetic abnormality observed after loss of β-, γ1-, or β- and γ1-synucleins is attributable to loss of synucleins rather than an artifact of the experimental system. Together, these findings demonstrate that β- and γ1-synuclein expression in neurons is essential for physiological functions that underlie normal motor behavior during development.

β- and γ1-Synucleins Are Required for Development of the Dopamine System—We next addressed the hypothesis that the motor phenotype resulting from loss of β- or γ1-synuclein was attributable to abnormalities of the dopamine system. We first asked whether development of dopaminergic neurons differed between controls and zebrafish lacking β-, γ1-, or both synucleins. RNA *in situ* hybridization was carried out at 48, 72, and 96 hpf, using a cRNA probe to *slc6a3* (dopamine transporter, *dat*), which is specifically expressed in dopamine neurons (38, 46) (Fig. 7*A*). No qualitative differences were observed in the distribution or staining intensity of *slc6a3*-expressing cells between controls and larvae lacking β-, γ1-, or both synucleins. However, quantification by an observer blinded to MO exposure showed a modest reduction in the number of *slc6a3*$^+$ cells in larvae lacking both β- and γ1-synucleins at 48 hpf (Fig. 7*B*). This abnormality had recovered by 72 hpf, such that there was no difference in the number of *slc6a3*$^+$ cells between WT larvae and those exposed to β + γ1 MO (Fig. 7*C*). Expression of GFP or human α-synuclein did not alter the number of *slc6a3*$^+$ neurons in control larvae (Fig. 7*D*). However, expression of human α-synuclein was sufficient to prevent a reduction in the number of *slc6a3*$^+$ cells in the absence of β- and γ1-synucleins, whereas GFP expression did not rescue this phenotype. These data show that both β- and γ1-synuclein are necessary for early development or differentiation of dopamine neurons. However, there was a normal complement of dopamine neurons by 4 dpf, when the hypokinetic phenotype in zebrafish lacking synucleins was most prominent.

Downloaded from http://www.jbc.org/ at ERASMUS MC on March 27, 2018

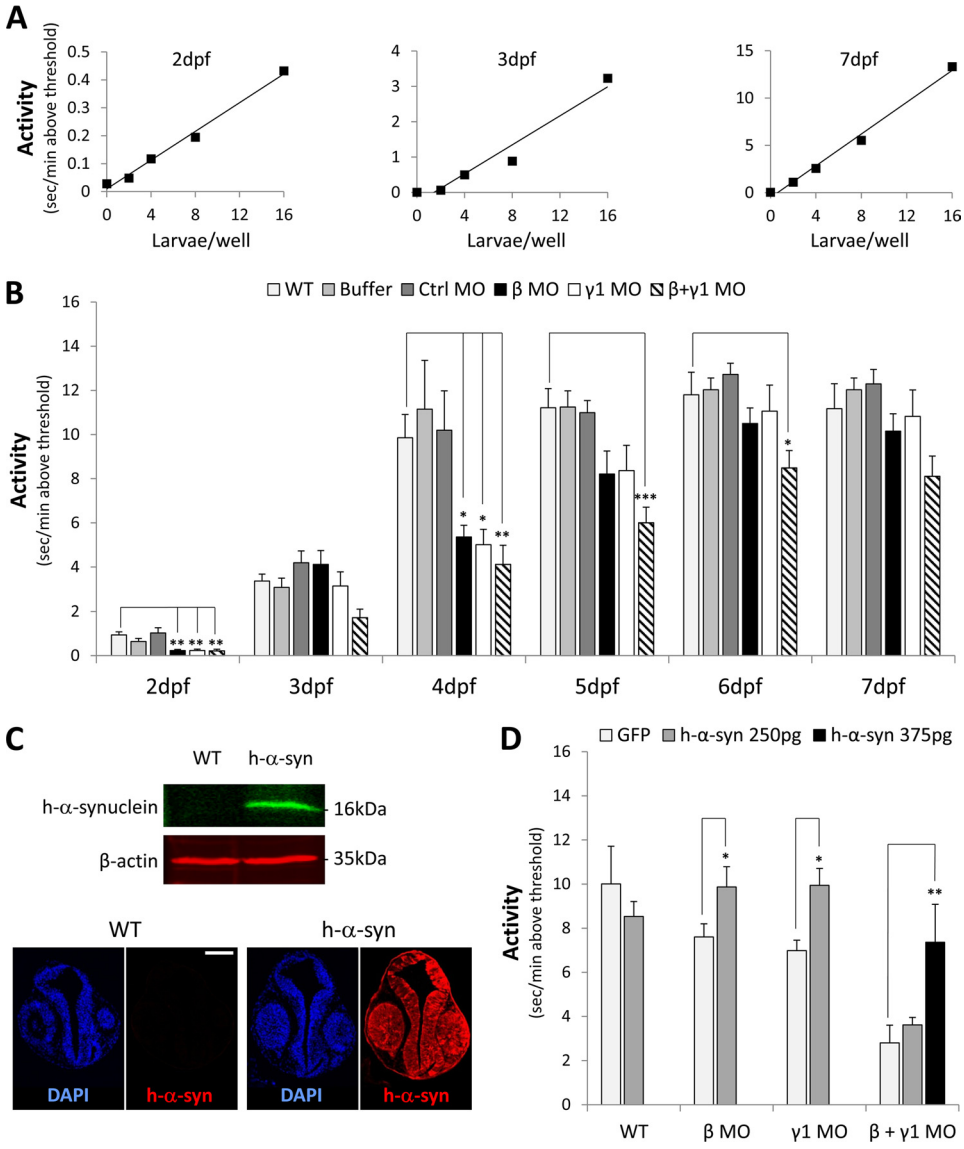

FIGURE 6. **Spontaneous movement is impaired in zebrafish lacking β- or γ1-synucleins.** *A*, assay validation. Standard curves were constructed to investigate the linearity of measurement of spontaneous motor activity using a pixel quantification method. 0, 2, 4, 8, or 16 larvae were recorded moving spontaneously in the wells of a 12-well plate at 2, 3, or 7 dpf, and their movement was quantified by measuring the proportion of successive video frames in which changes in pixel gray scale values exceeded the threshold for detection of movement above noise. *B*, spontaneous motor activity was quantified in groups of 15 zebrafish larvae moving in the wells of 12-well plates between days 2 and 7 postfertilization. Uninjected controls (*WT*) were compared with larvae that were injected at the single cell stage with injection buffer only (*Buffer*), a non-targeting MO control (*Ctrl MO*), or MOs targeting *sncb* (*β MO*), *sncg1* (*γ1 MO*), or *sncb* and *sncg1* (*β + γ1 MO*). The mean values of six independent experimental replicates are shown for each data point. *Error bars*, S.E. Statistically significant differences between controls and MO-treated larvae are shown (*, $p < 0.05$; **, $p < 0.01$; ***, $p < 0.001$, one-way ANOVA, Dunnet's *post hoc* test). *C*, *top*, Western blot of lysates from pooled 24-hpf whole zebrafish. Wild-type embryos were compared with embryos microinjected with human α-synuclein-IRES-GFP mRNA. The blot was simultaneously probed with antibodies to human α-synuclein (*green*, *top image*) and β-actin (*red*, *bottom image*) as a loading control. *C*, *bottom*, sections of the developing head region from 24-hpf zebrafish stained for nuclei (DAPI, *blue*) to illustrate the anatomy and α-synuclein (*red*) to confirm expression in the developing neural tube and retina. *D*, spontaneous motor activity was quantified in groups of 15 zebrafish larvae moving in the wells of 12-well plates at day 4 post-fertilization. Embryos were injected at the single cell stage with control GFP mRNA (250 pg, *light gray bars*) or human α-synuclein-IRES-GFP mRNA (250 pg (*dark gray bars*) or 375 pg (*black bars*)), following by MOs targeting *sncb* (*β MO*), *sncg1* (*γ1 MO*), or *sncb* and *sncg1* (*β + γ1 MO*). WT controls were injected with mRNA but did not receive MO. The mean values of six independent experimental replicates are shown for each data point. *Error bars*, S.E. Statistically significant differences are shown between larvae expressing GFP and α-synuclein (*, $p < 0.05$; **, $p < 0.01$, one-way ANOVA, Dunnet's *post hoc* test).

Finally, we asked whether abnormalities of monoaminergic neurochemistry might explain the hypokinesia resulting from loss of β- or γ1-synucleins. We examined steady-state whole larval dopamine levels at 7 dpf, which was the earliest time point at which we could measure neurotransmitters with sufficiently low variability to enable detection of differences between multiple experimental groups. Although gene expression had recovered by this time point, zebrafish lacking both β- and γ1-synucleins earlier in development showed significantly reduced dopamine levels at 7 dpf compared with Ctrl MO-injected animals (Fig. 7*E*). None of the other experimental groups showed significant differences from controls. Transient expression of GFP or human α-synuclein early in development did not change steady state levels of dopamine in WT larvae at 7 dpf. However, α-synuclein but not GFP prevented the loss of dopamine that occurred in the absence of zebrafish β- and γ1-sy-

Downloaded from http://www.jbc.org/ at ERASMUS MC on March 27, 2018

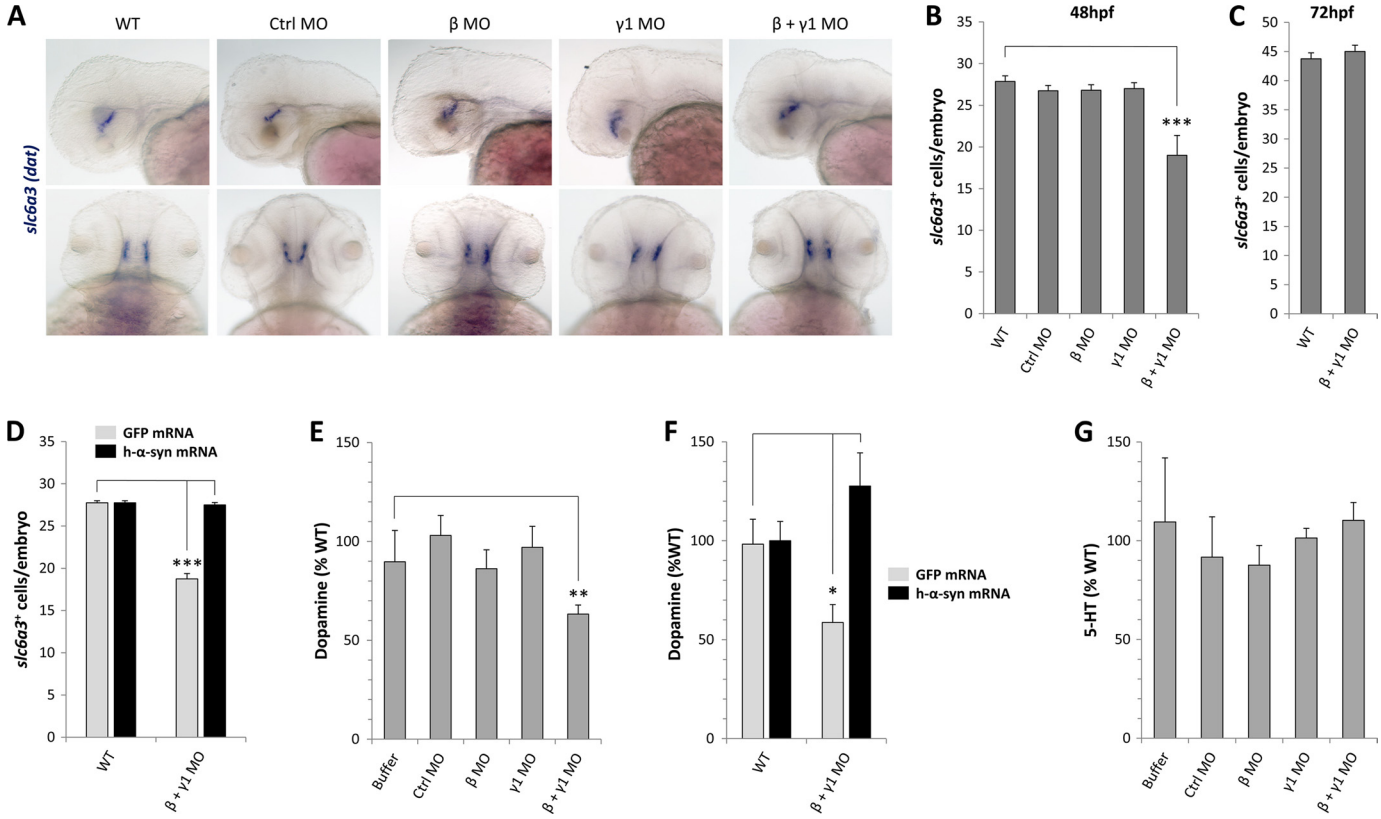

FIGURE 7. **The dopamine system in zebrafish lacking β- or γ1-synucleins.** *A*, whole mount RNA *in situ* hybridization was carried out using a probe to *slc6a3* (dopamine transporter, *dat*) to label dopaminergic neurons; hybridized probe was revealed using a chromogenic reaction with a *blue/purple* product. The images show lateral (*top row*) and dorsal (*bottom row*) photographs of the head regions of zebrafish at 48 hpf. Uninjected controls (*WT*) were compared with larvae that were injected at the single cell stage with a non-targeting MO control (*Ctrl MO*), and MOs targeting *sncb* (*β MO*), *sncg1* (*γ1 MO*), or *sncb* and *sncg1* (*β + γ1 MO*). *B* and *C*, the number of dopamine neurons in larvae from each group (uninjected controls, non-targeting control MO, β MO, γ1 MO, and β + γ1 MO) was counted manually at 48 hpf (*B*) and 72 hpf (*C*). The mean of six embryos in each group is shown. *Error bars*, S.E. (***, $p < 0.001$, one-way ANOVA, Dunnet's post hoc test WT *versus* β + γ1 MO). *D*, mRNA rescue control. Embryos were injected at the single cell stage with GFP control mRNA (250 pg, *light gray bars*), or human α-synuclein-IRES-GFP mRNA (250 pg, *black bars*), followed by MOs targeting *sncb* and *sncg1* (*β + γ1 MO*), or no MO (*WT*). The number of dopamine neurons in larvae from each group was counted manually at 48 hpf. The mean of six embryos in each group is shown; *error bars* show the S.E. (***$p <$ 0.001, one-way ANOVA, Dunnet's post hoc test, β + γ1 MO/GFP *versus* β + γ1 MO/α-synuclein and WT/GFP *versus* β + γ1 MO/GFP). *E*, whole larval dopamine levels were measured at 7 dpf in samples of 30 larvae from each group (uninjected controls, buffer injection only, non-targeting control MO, β MO, γ1 MO, and β + γ1 MO) and normalized to the value for uninjected controls. The mean of three independent experiments is shown; *error bars* show the S.E. (**, $p < 0.01$, one-way ANOVA, Dunnet's post hoc test, WT *versus* β + γ1 MO). *F*, mRNA rescue control. Embryos were injected at the single cell stage with GFP control mRNA (250 pg, *light gray bars*) or human α-synuclein-IRES-GFP mRNA (250 pg, *black bars*), followed by MOs targeting *sncb* and *sncg1* (β + γ1 MO), or no MO (*WT*). Whole larval dopamine levels were measured at 7 dpf in samples of 30 larvae from each group and normalized to the value for uninjected controls. The mean of three independent experiments is shown; *error bars* show the S.E. (**, $p < 0.01$, one-way ANOVA, Dunnet's post hoc test, β + γ1 MO/GFP *versus* β + γ1 MO/human α-synuclein, and WT/GFP *versus* β + γ1 MO/GFP). *G*, whole larval 5-hydroxytryptamine (*5-HT*) levels were measured at 7 dpf in samples of 30 larvae from each group (uninjected controls, buffer injection only, non-targeting control MO, β MO, γ1 MO, β + γ1 MO) and normalized to the value for WT larvae. The mean of three independent experiments is shown. *Error bars*, S.E.

nucleins (Fig. 7*F*). These data show that early developmental expression of both β- and γ1-synucleins is necessary for establishment of normal dopamine levels. Interestingly, 5-hydroxytryptamine levels were not reduced in larvae lacking synucleins (Fig. 7*G*), suggesting that the relevant function of synucleins in this context may be specific to dopaminergic neurons.

DISCUSSION

A genomic duplication occurred early in the evolution of ray-finned fish (47) and probably accounts for the presence of two *sncg* genes in zebrafish, similar to fugu, medaka, salmon, and stickleback (48). In some cases, duplicated genes have complementary roles, sharing multiple functions of the ancestral gene (49). The dual zebrafish paralogues of γ-synuclein show distinct temporal and spatial expression patterns; this may have allowed segregation of neural and non-neural functions of γ-synuclein into separate proteins and provided evolutionary pressure to retain both genes. Conversely, our data suggest that an ancestral *snca* gene and its flanking genes were lost during zebrafish evolution. The putative deletion appears to have occurred more recently than the duplication of *sncg*, because a number of other fish species, including salmon and fugu, harbor duplicate *sncg* genes in addition to *snca* and *sncb*. A precedent for spontaneous loss of *snca* has been described in a subpopulation of the C57BL/6J strain of mice that developed a *de novo* deletion of the *SNCA* locus (15). It is likely that other synuclein family members provide compensatory functions accommodating the loss of a single synuclein gene; mice lacking α-, β-, and γ-synucleins (20–22) showed more severe phenotypes than animals lacking one or two synucleins (17, 18), and abnormalities in α-, β-, and γ-synuclein null mice were mitigated by expression of human α-synuclein (21). Here we provide further evidence of cross-functionality between dif-

Downloaded from http://www.jbc.org/ at ERASMUS MC on March 27, 2018

ferent synucleins by showing that loss of zebrafish β- and γ1-synucleins gave rise to a more severe phenotype than loss of one or other synuclein and that abnormalities arising from loss of either protein were rescued by expression of human α-synuclein.

By using an assay sensitive to motor function early in development, we demonstrated that transient abrogation of β- or γ1-synuclein expression suppressed normal spontaneous motor activity in larval zebrafish. There was no accompanying alteration in the structure of the body or CNS, and we conclude that the mechanisms underlying the observed hypokinesia are likely to involve a disturbance of neuronal function. Resolution of hypokinesia was temporally correlated with the gradual recovery of gene expression after 72–96 hpf, suggesting that synucleins dynamically regulate aspects of neuronal function governing initiation of spontaneous movement. Abnormalities of synaptic transmission have been demonstrated in murine synuclein knock-out models (20, 21), and it is possible that similar defects arise in circuits mediating initiation of spontaneous movement in zebrafish lacking β- or γ1-synucleins. Given the importance of dopaminergic mechanisms in human hypokinetic movement disorders associated with synucleinopathy and the possibility that synucleins have important specific functions in dopamine neurons (22), we evaluated the role of β- and γ1-synucleins in the dopaminergic system. Both proteins were expressed in dopamine neurons throughout the CNS, and loss of both proteins delayed the appearance of a full complement of *slc6a3*$^{+}$-expressing neurons in the developing brain. Although the number of *slc6a3*$^{+}$-neurons was normal at 4 dpf, it is possible that delayed differentiation of dopaminergic neurons might contribute to later abnormalities of motility, by affecting the formation of motor circuits. Even in the presence of a normal number of dopamine neurons, we found evidence of disturbed dopaminergic function; at 7 dpf, zebrafish exposed to β + γ1 MOs showed decreased dopamine levels, similar to previous studies in synuclein gene knock-out mice (17, 22). Because reproducible measurements of dopamine levels were not technically feasible at earlier time points, we did not exclude the possibility that reduced dopamine levels were also present at the time points where the most prominent hypokinesia was observed. The development of zebrafish lines harboring stable null alleles of *sncb* and *sncg1* will allow clarification of the relationship between synucleins, dopamine levels, and motor phenotypes later in development when neurochemical measurements are more robust. Stable *sncb*$^{-/-}$ and *sncg1*$^{-/-}$ lines will also allow unbiased screening approaches to isolate modifiers of the hypokinetic synuclein-null phenotype that might be informative concerning genetic interactions of synucleins in vertebrate neurons *in vivo*. Previous screens for genetic modifiers have been carried out in yeast expressing human α-synuclein (50–52), and the role of a subset of identified modifiers was confirmed in fly (53) and worm (52) models. Although these studies provide information about the pathways involved in cellular responses to ectopic α-synuclein overexpression, the physiological roles of synucleins may depend on specific protein interactions absent from organisms lacking synucleins natively. Consequently, zebrafish models may contribute important new insights into synuclein function at the vertebrate presynaptic terminal.

There has been increasing interest in the development of zebrafish models of human neurological disease for therapeutic target identification and drug discovery *in vivo* (28). Transient knockdown of a number of different zebrafish orthologues of human genes implicated in parkinsonism resulted in dopaminergic phenotypes, including loss of neurons (54–56), altered function (56), or susceptibility to toxins (55, 57). Furthermore, zebrafish exposed to toxins implicated in PD pathogenesis (41, 58–61) showed loss of dopamine neurons, dopamine content, or dopaminergic function. Together, these data have provided encouragement that it might be possible to recapitulate aspects of PD pathogenesis accurately in zebrafish, an essential prerequisite for the development of useful models. We report here that zebrafish lack endogenous α-synuclein, which may cast doubt on whether key aspects of PD pathogenesis can be reproduced in a zebrafish model. α-Synuclein pathology is not prominent in some types of PD (62, 63), and it is currently unclear whether α-synuclein is necessary for PD pathogenesis in all cases. However, we consider the construction of transgenic zebrafish lines expressing physiological levels of human or fish α-synucleins an important priority. Because the zebrafish natively presents an *snca*-null background, comparison of α-synuclein-expressing transgenic lines with controls should clarify the role of α-synuclein in neuronal loss caused by PD-relevant environmental and genetic triggers.

REFERENCES

1. Clayton, D. F., and George, J. M. (1998) The synucleins. A family of proteins involved in synaptic function, plasticity, neurodegeneration, and disease. *Trends Neurosci.* **21,** 249–254
2. Polymeropoulos, M. H., Lavedan, C., Leroy, E., Ide, S. E., Dehejia, A., Dutra, A., Pike, B., Root, H., Rubenstein, J., Boyer, R., Stenroos, E. S., Chandrasekharappa, S., Athanassiadou, A., Papapetropoulos, T., Johnson, W. G., Lazzarini, A. M., Duvoisin, R. C., Di Iorio, G., Golbe, L. I., and Nussbaum, R. L. (1997) Mutation in the α-synuclein gene identified in families with Parkinson's disease. *Science* **276,** 2045–2047
3. Krüger, R., Kuhn, W., Müller, T., Woitalla, D., Graeber, M., Kösel, S., Przuntek, H., Epplen, J. T., Schöls, L., and Riess, O. (1998) Ala30Pro mutation in the gene encoding α-synuclein in Parkinson's disease. *Nat. Genet.* **18,** 106–108
4. Zarranz, J. J., Alegre, J., Gómez-Esteban, J. C., Lezcano, E., Ros, R., Ampuero, I., Vidal, L., Hoenicka, J., Rodriguez, O., Atarés, B., Llorens, V., Gomez Tortosa, E., del Ser, T., Muñoz, D. G., and de Yebenes, J. G. (2004) The new mutation, E46K, of α-synuclein causes Parkinson and Lewy body dementia. *Ann. Neurol.* **55,** 164–173
5. Singleton, A. B., Farrer, M., Johnson, J., Singleton, A., Hague, S., Kachergus, J., Hulihan, M., Peuralinna, T., Dutra, A., Nussbaum, R., Lincoln, S., Crawley, A., Hanson, M., Maraganore, D., Adler, C., Cookson, M. R., Muenter, M., Baptista, M., Miller, D., Blancato, J., Hardy, J., and Gwinn-Hardy, K. (2003) α-Synuclein locus triplication causes Parkinson's disease. *Science* **302,** 841
6. Chartier-Harlin, M. C., Kachergus, J., Roumier, C., Mouroux, V., Douay, X., Lincoln, S., Levecque, C., Larvor, L., Andrieux, J., Hulihan, M., Waucquier, N., Defebvre, L., Amouyel, P., Farrer, M., and Destée, A. (2004) α-Synuclein locus duplication as a cause of familial Parkinson's disease. *Lancet* **364,** 1167–1169
7. Spillantini, M. G., Schmidt, M. L., Lee, V. M., Trojanowski, J. Q., Jakes, R., and Goedert, M. (1997) α-Synuclein in Lewy bodies. *Nature* **388,** 839–840
8. Satake, W., Nakabayashi, Y., Mizuta, I., Hirota, Y., Ito, C., Kubo, M., Kawaguchi, T., Tsunoda, T., Watanabe, M., Takeda, A., Tomiyama, H., Na-

Downloaded from http://www.jbc.org/ at ERASMUS MC on March 27, 2018

kashima, K., Hasegawa, K., Obata, F., Yoshikawa, T., Kawakami, H., Sakoda, S., Yamamoto, M., Hattori, N., Murata, M., Nakamura, Y., and Toda, T. (2009) Genome-wide association study identifies common variants at four loci as genetic risk factors for Parkinson's disease. *Nat. Genet.* **41,** 1303–1307

9. Simón-Sánchez, J., Schulte, C., Bras, J. M., Sharma, M., Gibbs, J. R., Berg, D., Paisan-Ruiz, C., Lichtner, P., Scholz, S. W., Hernandez, D. G., Krüger, R., Federoff, M., Klein, C., Goate, A., Perlmutter, J., Bonin, M., Nalls, M. A., Illig, T., Gieger, C., Houlden, H., Steffens, M., Okun, M. S., Racette, B. A., Cookson, M. R., Foote, K. D., Fernandez, H. H., Traynor, B. J., Schreiber, S., Arepalli, S., Zonozi, R., Gwinn, K., van der Brug, M., Lopez, G., Chanock, S. J., Schatzkin, A., Park, Y., Hollenbeck, A., Gao, J., Huang, X., Wood, N. W., Lorenz, D., Deuschl, G., Chen, H., Riess, O., Hardy, J. A., Singleton, A. B., and Gasser, T. (2009) Genome-wide association study reveals genetic risk underlying Parkinson's disease. *Nat. Genet.* **41,** 1308–1312
10. Edwards, T. L., Scott, W. K., Almonte, C., Burt, A., Powell, E. H., Beecham, G. W., Wang, L., Züchner, S., Konidari, I., Wang, G., Singer, C., Nahab, F., Scott, B., Stajich, J. M., Pericak-Vance, M., Haines, J., Vance, J. M., and Martin, E. R. (2010) Genome-wide association study confirms SNPs in SNCA and the MAPT region as common risk factors for Parkinson disease. *Ann. Hum. Genet.* **74,** 97–109
11. Fuchs, J., Tichopad, A., Golub, Y., Munz, M., Schweitzer, K. J., Wolf, B., Berg, D., Mueller, J. C., and Gasser, T. (2008) Genetic variability in the SNCA gene influences α-synuclein levels in the blood and brain. *FASEB J.* **22,** 1327–1334
12. Schlüter, O. M., Fornai, F., Alessandrí, M. G., Takamori, S., Geppert, M., Jahn, R., and Südhof, T. C. (2003) Role of α-synuclein in 1-methyl-4-phenyl-1,2,3,6-tetrahydropyridine-induced parkinsonism in mice. *Neuroscience* **118,** 985–1002
13. Dauer, W., Kholodilov, N., Vila, M., Trillat, A. C., Goodchild, R., Larsen, K. E., Staal, R., Tieu, K., Schmitz, Y., Yuan, C. A., Rocha, M., Jackson-Lewis, V., Hersch, S., Sulzer, D., Przedborski, S., Burke, R., and Hen, R. (2002) Resistance of α-synuclein null mice to the parkinsonian neurotoxin MPTP. *Proc. Natl. Acad. Sci. U.S.A.* **99,** 14524–14529
14. Abeliovich, A., Schmitz, Y., Fariñas, I., Choi-Lundberg, D., Ho, W. H., Castillo, P. E., Shinsky, N., Verdugo, J. M., Armanini, M., Ryan, A., Hynes, M., Phillips, H., Sulzer, D., and Rosenthal, A. (2000) Mice lacking α-synuclein display functional deficits in the nigrostriatal dopamine system. *Neuron* **25,** 239–252
15. Specht, C. G., and Schoepfer, R. (2001) Deletion of the α-synuclein locus in a subpopulation of C57BL/6J inbred mice. *BMC Neurosci.* **2,** 11
16. Cabin, D. E., Shimazu, K., Murphy, D., Cole, N. B., Gottschalk, W., McIlwain, K. L., Orrison, B., Chen, A., Ellis, C. E., Paylor, R., Lu, B., and Nussbaum, R. L. (2002) Synaptic vesicle depletion correlates with attenuated synaptic responses to prolonged repetitive stimulation in mice lacking α-synuclein. *J. Neurosci.* **22,** 8797–8807
17. Chandra, S., Fornai, F., Kwon, H. B., Yazdani, U., Atasoy, D., Liu, X., Hammer, R. E., Battaglia, G., German, D. C., Castillo, P. E., and Südhof, T. C. (2004) Double-knockout mice for α- and β-synucleins. Effect on synaptic functions. *Proc. Natl. Acad. Sci. U.S.A.* **101,** 14966–14971
18. Ninkina, N., Papachroni, K., Robertson, D. C., Schmidt, O., Delaney, L., O'Neill, F., Court, F., Rosenthal, A., Fleetwood-Walker, S. M., Davies, A. M., and Buchman, V. L. (2003) Neurons expressing the highest levels of γ-synuclein are unaffected by targeted inactivation of the gene. *Mol. Cell Biol.* **23,** 8233–8245
19. Robertson, D. C., Schmidt, O., Ninkina, N., Jones, P. A., Sharkey, J., and Buchman, V. L. (2004) Developmental loss and resistance to MPTP toxicity of dopaminergic neurones in substantia nigra pars compacta of γ-synuclein, α-synuclein and double α/γ-synuclein null mutant mice. *J. Neurochem.* **89,** 1126–1136
20. Greten-Harrison, B., Polydoro, M., Morimoto-Tomita, M., Diao, L., Williams, A. M., Nie, E. H., Makani, S., Tian, N., Castillo, P. E., Buchman, V. L., and Chandra, S. S. (2010) αβγ-Synuclein triple knockout mice reveal age-dependent neuronal dysfunction. *Proc. Natl. Acad. Sci. U.S.A.* **107,** 19573–19578
21. Burré, J., Sharma, M., Tsetsenis, T., Buchman, V., Etherton, M. R., and Südhof, T. C. (2010) α-synuclein promotes SNARE complex assembly *in vivo* and *in vitro*. *Science* **329,** 1663–1667
22. Anwar, S., Peters, O., Millership, S., Ninkina, N., Doig, N., Connor-Robson, N., Threlfell, S., Kooner, G., Deacon, R. M., Bannerman, D. M., Bolam, J. P., Chandra, S. S., Cragg, S. J., Wade-Martins, R., and Buchman, V. L. (2011) Functional alterations to the nigrostriatal system in mice lacking all three members of the synuclein family. *J. Neurosci.* **31,** 7264–7274
23. Park, H. C., Kim, C. H., Bae, Y. K., Yeo, S. Y., Kim, S. H., Hong, S. K., Shin, J., Yoo, K. W., Hibi, M., Hirano, T., Miki, N., Chitnis, A. B., and Huh, T. L. (2000) Analysis of upstream elements in the HuC promoter leads to the establishment of transgenic zebrafish with fluorescent neurons. *Dev. Biol.* **227,** 279–293
24. Bai, Q., Garver, J. A., Hukriede, N. A., and Burton, E. A. (2007) Generation of a transgenic zebrafish model of Tauopathy using a novel promoter element derived from the zebrafish *eno2* gene. *Nucleic Acids Res.* **35,** 6501–6516
25. McLean, D. L., and Fetcho, J. R. (2009) Spinal interneurons differentiate sequentially from those driving the fastest swimming movements in larval zebrafish to those driving the slowest ones. *J. Neurosci.* **29,** 13566–13577
26. Muto, A., Ohkura, M., Kotani, T., Higashijima, S., Nakai, J., and Kawakami, K. (2011) Genetic visualization with an improved GCaMP calcium indicator reveals spatiotemporal activation of the spinal motor neurons in zebrafish. *Proc. Natl. Acad. Sci. U.S.A.* **108,** 5425–5430
27. Naumann, E. A., Kampff, A. R., Prober, D. A., Schier, A. F., and Engert, F. (2010) Monitoring neural activity with bioluminescence during natural behavior. *Nat. Neurosci.* **13,** 513–520
28. Bandmann, O., and Burton, E. A. (2010) Genetic zebrafish models of neurodegenerative diseases. *Neurobiol. Dis.* **40,** 58–65
29. Panula, P., Chen, Y. C., Priyadarshini, M., Kudo, H., Semenova, S., Sundvik, M., and Sallinen, V. (2010) The comparative neuroanatomy and neurochemistry of zebrafish CNS systems of relevance to human neuropsychiatric diseases. *Neurobiol. Dis.* **40,** 46–57
30. Sager, J. J., Bai, Q., and Burton, E. A. (2010) Transgenic zebrafish models of neurodegenerative diseases. *Brain Struct. Funct.* **214,** 285–302
31. Mullins, M. C., Hammerschmidt, M., Haffter, P., and Nüsslein-Volhard, C. (1994) Large-scale mutagenesis in the zebrafish. In search of genes controlling development in a vertebrate. *Curr. Biol.* **4,** 189–202
32. Amsterdam, A., Burgess, S., Golling, G., Chen, W., Sun, Z., Townsend, K., Farrington, S., Haldi, M., and Hopkins, N. (1999) A large-scale insertional mutagenesis screen in zebrafish. *Genes Dev.* **13,** 2713–2724
33. Zon, L. I., and Peterson, R. T. (2005) *In vivo* drug discovery in the zebrafish. *Nat. Rev. Drug Discov.* **4,** 35–44
34. Rihel, J., Prober, D. A., Arvanites, A., Lam, K., Zimmerman, S., Jang, S., Haggarty, S. J., Kokel, D., Rubin, L. L., Peterson, R. T., and Schier, A. F. (2010) Zebrafish behavioral profiling links drugs to biological targets and rest/wake regulation. *Science* **327,** 348–351
35. Sinha, A. U., and Meller, J. (2007) Cinteny. Flexible analysis and visualization of synteny and genome rearrangements in multiple organisms. *BMC Bioinformatics* **8,** 82
36. Bai, Q., Mullett, S. J., Garver, J. A., Hinkle, D. A., and Burton, E. A. (2006) Zebrafish DJ-1 is evolutionarily conserved and expressed in dopaminergic neurons. *Brain Res.* **1113,** 33–44
37. Bai, Q., Wei, X., and Burton, E. A. (2009) Expression of a 12-kb promoter element derived from the zebrafish enolase-2 gene in the zebrafish visual system. *Neurosci. Lett.* **449,** 252–257
38. Bai, Q., and Burton, E. A. (2009) Cis-acting elements responsible for dopaminergic neuron-specific expression of zebrafish slc6a3 (dopamine transporter) *in vivo* are located remote from the transcriptional start site. *Neuroscience* **164,** 1138–1151
39. Bai, Q., Sun, M., Stolz, D. B., and Burton, E. A. (2011) Major isoform of zebrafish P0 is a 23.5-kDa myelin glycoprotein expressed in selected white matter tracts of the central nervous system. *J. Comp. Neurol.* **519,** 1580–1596
40. Turner, D. L., and Weintraub, H. (1994) Expression of achaete-scute homolog 3 in *Xenopus* embryos converts ectodermal cells to a neural fate. *Genes Dev.* **8,** 1434–1447
41. Sallinen, V., Torkko, V., Sundvik, M., Reenilä, I., Khrustalyov, D., Kaslin, J., and Panula, P. (2009) MPTP and MPP^+ target specific aminergic cell populations in larval zebrafish. *J. Neurochem.* **108,** 719–731
42. Sun, Z., and Gitler, A. D. (2008) Discovery and characterization of three

Downloaded from http://www.jbc.org/ at ERASMUS MC on March 27, 2018

novel synuclein genes in zebrafish. *Dev. Dyn.* **237,** 2490–2495
43. Chen, Y. C., Cheng, C. H., Chen, G. D., Hung, C. C., Yang, C. H., Hwang, S. P., Kawakami, K., Wu, B. K., and Huang, C. J. (2009) Recapitulation of zebrafish sncga expression pattern and labeling the habenular complex in transgenic zebrafish using green fluorescent protein reporter gene. *Dev. Dyn.* **238,** 746–754
44. Lo, K., and Smale, S. T. (1996) Generality of a functional initiator consensus sequence. *Gene* **182,** 13–22
45. Thisse, C., and Thisse, B. (2004) Fast Release Clones: A High Throughput Expression Analysis. in *ZFIN*, ZDB-PUB-040907-1, University of Oregon, Eugene, OR
46. Holzschuh, J., Ryu, S., Aberger, F., and Driever, W. (2001) Dopamine transporter expression distinguishes dopaminergic neurons from other catecholaminergic neurons in the developing zebrafish embryo. *Mech. Dev.* **101,** 237–243
47. Amores, A., Force, A., Yan, Y. L., Joly, L., Amemiya, C., Fritz, A., Ho, R. K., Langeland, J., Prince, V., Wang, Y. L., Westerfield, M., Ekker, M., and Postlethwait, J. H. (1998) Zebrafish hox clusters and vertebrate genome evolution. *Science* **282,** 1711–1714
48. Yoshida, H., Craxton, M., Jakes, R., Zibaee, S., Tavaré, R., Fraser, G., Serpell, L. C., Davletov, B., Crowther, R. A., and Goedert, M. (2006) Synuclein proteins of the pufferfish *Fugu rubripes*. Sequences and functional characterization. *Biochemistry* **45,** 2599–2607
49. Lepiller, S., Franche, N., Solary, E., Chluba, J., and Laurens, V. (2009) Comparative analysis of zebrafish *nos2a* and *nos2b* genes. *Gene* **445,** 58–65
50. Cooper, A. A., Gitler, A. D., Cashikar, A., Haynes, C. M., Hill, K. J., Bhullar, B., Liu, K., Xu, K., Strathearn, K. E., Liu, F., Cao, S., Caldwell, K. A., Caldwell, G. A., Marsischky, G., Kolodner, R. D., Labaer, J., Rochet, J. C., Bonini, N. M., and Lindquist, S. (2006) α-Synuclein blocks ER-Golgi traffic and Rab1 rescues neuron loss in Parkinson models. *Science* **313,** 324–328
51. Liang, J., Clark-Dixon, C., Wang, S., Flower, T. R., Williams-Hart, T., Zweig, R., Robinson, L. C., Tatchell, K., and Witt, S. N. (2008) Novel suppressors of α-synuclein toxicity identified using yeast. *Hum. Mol. Genet.* **17,** 3784–3795
52. Willingham, S., Outeiro, T. F., DeVit, M. J., Lindquist, S. L., and Muchowski, P. J. (2003) Yeast genes that enhance the toxicity of a mutant huntingtin fragment or α-synuclein. *Science* **302,** 1769–1772
53. Trinh, K., Moore, K., Wes, P. D., Muchowski, P. J., Dey, J., Andrews, L., and Pallanck, L. J. (2008) Induction of the phase II detoxification pathway suppresses neuron loss in *Drosophila* models of Parkinson's disease. *J. Neurosci.* **28,** 465–472
54. Flinn, L., Mortiboys, H., Volkmann, K., Köster, R. W., Ingham, P. W., and Bandmann, O. (2009) Complex I deficiency and dopaminergic neuronal cell loss in parkin-deficient zebrafish (*Danio rerio*). *Brain* **132,** 1613–1623
55. Sallinen, V., Kolehmainen, J., Priyadarshini, M., Toleikyte, G., Chen, Y. C., and Panula, P. (2010) Dopaminergic cell damage and vulnerability to MPTP in Pink1 knockdown zebrafish. *Neurobiol. Dis.* **40,** 93–101
56. Sheng, D., Qu, D., Kwok, K. H., Ng, S. S., Lim, A. Y., Aw, S. S., Lee, C. W., Sung, W. K., Tan, E. K., Lufkin, T., Jesuthasan, S., Sinnakaruppan, M., and Liu, J. (2010) Deletion of the WD40 domain of LRRK2 in zebrafish causes parkinsonism-like loss of neurons and locomotive defect. *PLoS Genet.* **6,** e1000914
57. Bretaud, S., Allen, C., Ingham, P. W., and Bandmann, O. (2007) p53-dependent neuronal cell death in a DJ-1-deficient zebrafish model of Parkinson's disease. *J. Neurochem.* **100,** 1626–1635
58. Anichtchik, O. V., Kaslin, J., Peitsaro, N., Scheinin, M., and Panula, P. (2004) Neurochemical and behavioral changes in zebrafish *Danio rerio* after systemic administration of 6-hydroxydopamine and 1-methyl-4-phenyl-1,2,3,6-tetrahydropyridine. *J. Neurochem.* **88,** 443–453
59. Bretaud, S., Lee, S., and Guo, S. (2004) Sensitivity of zebrafish to environmental toxins implicated in Parkinson's disease. *Neurotoxicol. Teratol.* **26,** 857–864
60. Lam, C. S., Korzh, V., and Strahle, U. (2005) Zebrafish embryos are susceptible to the dopaminergic neurotoxin MPTP. *Eur. J. Neurosci.* **21,** 1758–1762
61. McKinley, E. T., Baranowski, T. C., Blavo, D. O., Cato, C., Doan, T. N., and Rubinstein, A. L. (2005) Neuroprotection of MPTP-induced toxicity in zebrafish dopaminergic neurons. *Brain Res. Mol. Brain Res.* **141,** 128–137
62. Hayashi, S., Wakabayashi, K., Ishikawa, A., Nagai, H., Saito, M., Maruyama, M., Takahashi, T., Ozawa, T., Tsuji, S., and Takahashi, H. (2000) An autopsy case of autosomal-recessive juvenile parkinsonism with a homozygous exon 4 deletion in the parkin gene. *Mov. Disord.* **15,** 884–888
63. Wider, C., Dickson, D. W., and Wszolek, Z. K. (2010) Leucine-rich repeat kinase 2 gene-associated disease. Redefining genotype-phenotype correlation. *Neurodegener. Dis.* **7,** 175–179
64. Ma, P. M. (2003) Catecholaminergic systems in the zebrafish. IV. Organization and projection pattern of dopaminergic neurons in the diencephalon. *J. Comp. Neurol.* **460,** 13–37

Downloaded from http://www.jbc.org/ at ERASMUS MC on March 27, 2018

Hypokinesia and Reduced Dopamine Levels in Zebrafish Lacking β- and γ 1-Synucleins

Chiara Milanese, Jonathan J. Sager, Qing Bai, Thomas C. Farrell, Jason R. Cannon, J. Timothy Greenamyre and Edward A. Burton

J. Biol. Chem. 2012, 287:2971-2983.
doi: 10.1074/jbc.M111.308312 originally published online November 29, 2011

Access the most updated version of this article at doi: 10.1074/jbc.M111.308312

Alerts:
- When this article is cited
- When a correction for this article is posted

Click here to choose from all of JBC's e-mail alerts

Supplemental material:
http://www.jbc.org/content/suppl/2011/11/29/M111.308312.DC1

This article cites 63 references, 19 of which can be accessed free at
http://www.jbc.org/content/287/5/2971.full.html#ref-list-1

Downloaded from http://www.jbc.org/ at ERASMUS MC on March 27, 2018